In-situ Synchrotron Radiation X-Ray Diffraction Study of Crystallization Kinetics of Polymorphs of 1,3-dioleoyl-2-palmitoyl glycerol (OPO)

Laura Bayés-García*,[a] Teresa Calvet,[a] Miquel Àngel Cuevas-Diarte,[a] Satoru Ueno,[b] and Kiyotaka Sato[b]

We examined the influence of kinetics on the polymorphic behavior of 1,3-dioleoyl-2-palmitoyl glycerol (OPO), a triacylglycerol (TAG) present in natural oils such as olive oil and human breast milk. Pure OPO was heated at
10 15°C·min⁻¹ in all cases. The polymorphic crystallization of OPO was studied at different cooling rates (15°, 2°, 1°, and 0.5°C·min⁻¹), and the dynamic polymorphic transformations were characterized on heating by simultaneously using Differential Scanning Calorimetry (DSC) and Synchrotron Radiation X-Ray Diffraction (SR-XRD) with small-angle X-ray diffraction (SAXD) and wide-angle X-ray diffraction (WAXD). Thermo-optical Microscopy (TOM) was also used in order to observe the polymorphic transitions. Polymorphic forms of OPO were identified and
15 characterized. As the cooling rate decreased, more stable forms crystallized, not following the Ostwald step rule, although in most cases concurrent crystallization occurred and the whole process was highly complex.

Introduction

Many crystals exhibit polymorphism, in which structural determination and thermodynamic stabilization of the
20 polymorphic modifications are of primary significance to determining the overall polymorphic nature of every substance.[1] In addition, the kinetic properties of crystallization and structural transformation are important, particularly for the application of polymorphic crystal systems
25 in pharmaceutical, biomedical, food technology, and other applications[2]. As for the crystallization of different polymorphic forms, the Ostwald step rule[3-6] has been used for macroscopic estimation of the behavior of multiple polymorphic forms when they are crystallized from vapor,
30 solution, and melt phases. This rule dictates that less stable polymorphic forms crystallize much faster than more stable forms when the driving force for crystallization takes place under certain values of supersaturation and supercooling and less stables forms transform to more stable forms after the
35 crystallization. Actually, the kinetics of polymorphic nucleation of various systems often follows this rule. For example, a metastable vaterite form crystallizes faster than the more stable calcite in $CaCO_3$.[7, 8] However, more detailed studies are needed to examine the effects of supercooling,
40 additives, etc. and becomes necessary to establish some rules of behavior of the influence of kinetics on the polymorphic crystallization and study the situations where the Ostwald step rule may be complemented.

Triacylglycerols (TAGs) are the main components of
45 alimentary fats and oils. Fat structures and compositions determine their physical properties[9, 10] (e.g., rheology, morphology, and texture), where polymorphism exerts a strong influence. Many studies have focused on the polymorphism of pure TAGs and binary mixtures[11-16] and the
50 influence of kinetics on polymorphic behavior.[17-21] The kinetics of fat crystallization is important to produce the desired product characteristics. Chong et al.[22] studied the influence of very low cooling rates on the crude palm oil crystallization in order to understand effects of cooling rates
55 on its fractionation. Roelands et al.[23] compared theoretical and experimentally determined nucleation rates in the precipitation processes of ionic and molecular compounds, and developed a standard procedure to measure them. Referring to isothermal crystallization kinetics, Foubert et
60 al.[24] describes a stop-and-return DSC method used in fat samples, which consists of stopping the crystallization at different moments during the isothermal crystallization and raising the temperature of the sample. However, Marangoni et al.[25] focused on nonisothermal nucleation of TAGs and
65 developed a model to estimate activation energy for nucleation in palm oil, milk fat, and other palm oil-based fats, defining the new parameter of supercooling-time exposure. Bouzidi et al.[26] used a model-free analysis of the kinetics of liquid-solid transformations for TAGs, and demonstrated the
70 existence of critical rates of cooling and specific growth modes. Moreover, Lam et al.[27] analyzed the influence of cooling rate on the formation of self-assembled fibrillar networks of 12 hydroxystearic acid (12HSA).

The present study analyzes a TAG (1,3-dioleoyl-2-palmitoyl
75 glycerol, OPO) that is important in palm oil fractionation,[28-30] as it belongs to low-melting temperature fractions. Palm oil is often modified to improve its applicability as an edible oil. Due to its heterogeneous composition, well-defined fractions with a high added value are obtained through fractionation.
80 Basically, dry fractionation consists of separating successively different crystal fractions obtained by controlled cooling from the melt. As the temperature decreases during fractionation, fractions richer in high levels of monounsaturated TAGs are separated. Minato et al.[12] studied the thermodynamic and
85 polymorphic behavior of OPO and 1,3-dipalmitoyl-2-oleoyl glycerol (POP) and their binary mixtures, showing the occurrence of α, β' and two β forms of OPO. However,
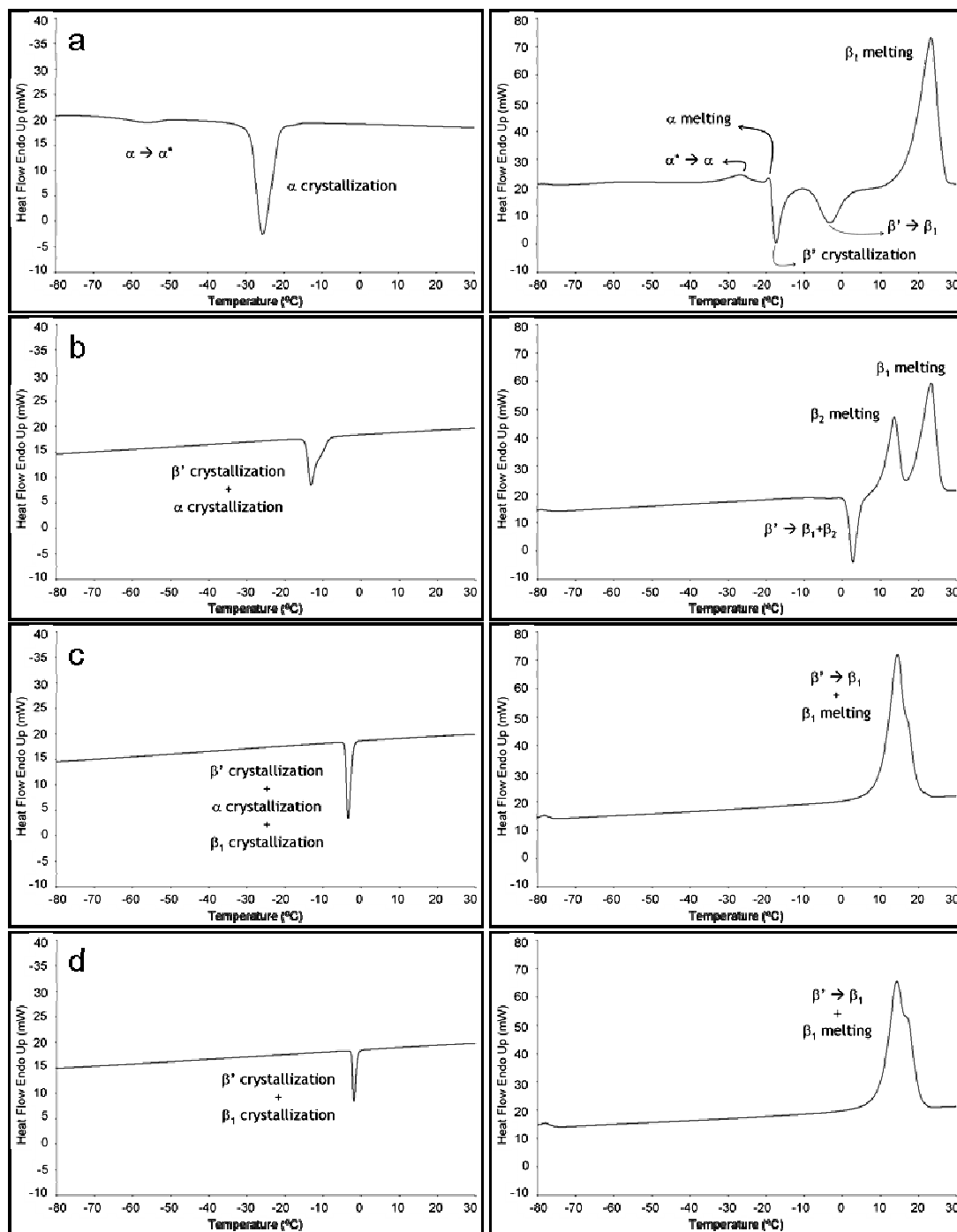
Figure 1. DSC thermograms of OPO obtained by changing the cooling rate and keeping a heating rate of 15º C·min^{-1}. a) Cooling profile at a rate of 15º C·min^{-1} and heating profile; b) Cooling profile at a rate of 2º C·min^{-1} and heating profile; c) Cooling profile at a rate of 1º C·min^{-1} and heating profile; d) Cooling profile at a rate of 0.5º C·min^{-1} and heating profile.

kinetic properties regarding to the crystallization rates of four forms of OPO at different cooling rates were not studied. The present work is focused on the influence of a kinetic parameter (cooling rate) on the polymorphic crystallization of (OPO). In particular, the relationship between this behavior and the Ostwald step rule is examined.

Synchrotron Radiation X-Ray Diffraction (SR-XRD) has been applied to the polymorphic transformations of TAGs.[17, 31, 32] Using this technique and Differential Scanning Calorimetry (DSC) enables rapid thermal programs to provide highly accurate structural information. However, few studies using SR-XRD have been conducted to determine the relative occurrence of the polymorphic forms of TAGs, since most work has been performed with an optical microscope, DSC,

Table 1. T_{onset} for each transition, obtained from the DSC data for OPO when the sample is cooled down at different cooling rates and heated at 15º C·min⁻¹

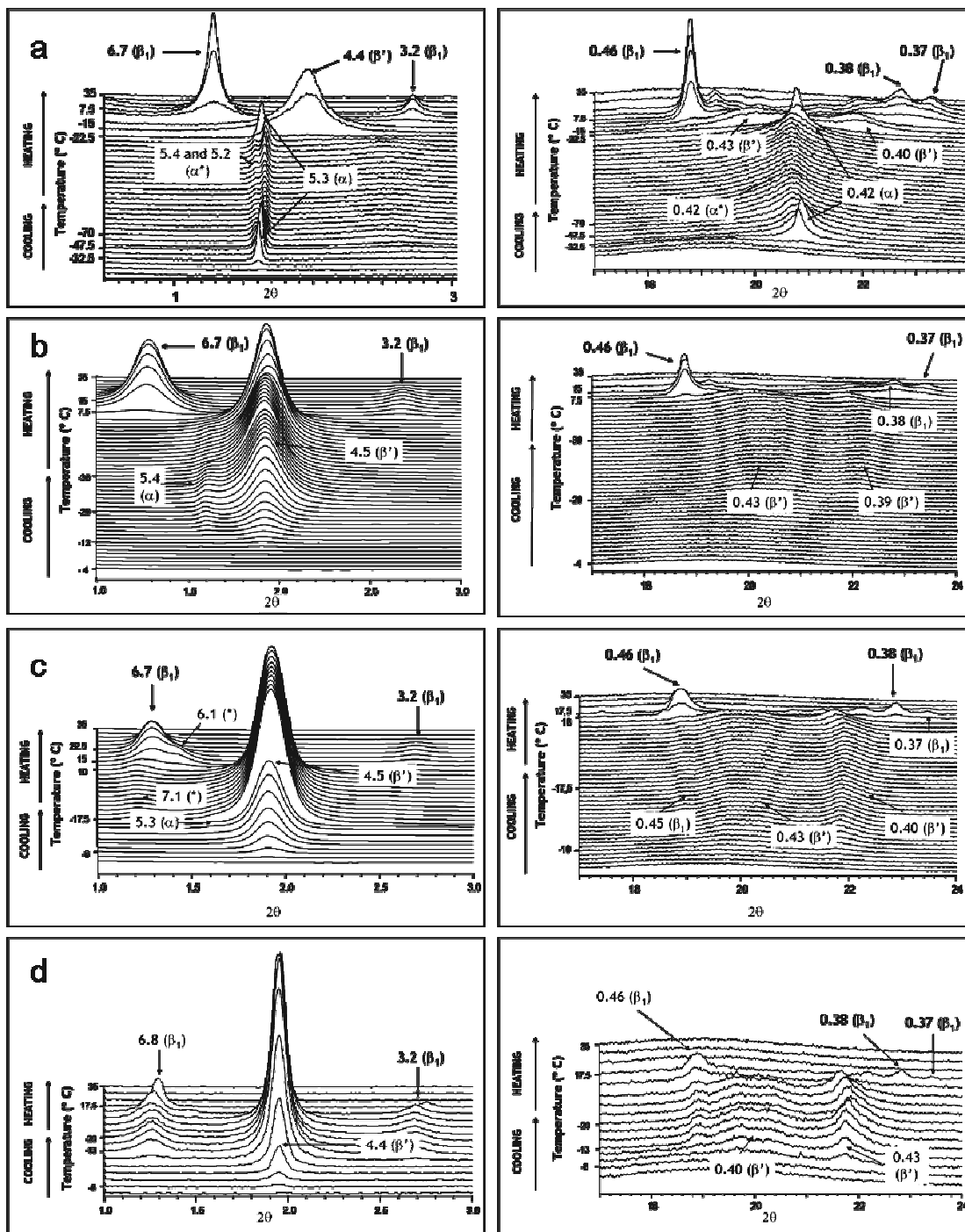| COOLING (rate: 15ºC·min⁻¹)		HEATING (rate: 15ºC·min⁻¹)				
α crystallization	α → α* transition	α* → α transition	α melting	β' crystallization	β' → β₁ transition	β₁ melting
T_{onset} (ºC)	T_{onset} (ºC)	T_{onset} (ºC)	T_{onset} (ºC)	T_{onset} (ºC)	T_{onset} (ºC)	T_{onset} (ºC)
-21.7 ± 0.3	-50.8 ± 1.6	-37.3 ± 0.4	-21.5 ± 0.3	-20.1 ± 0.3	-9.5 ± 0.3	13.6 ± 0.6
COOLING (rate: 2ºC·min⁻¹)		HEATING (rate: 15ºC·min⁻¹)				
Crystallization		β' → β₁ + β₂ transition		β₂ melting	β₁ melting	
T'_{onset} (ºC)	T_{onset} (ºC)	T_{onset} (ºC)		T_{onset} (ºC)	T_{onset} (ºC)	
-7.6 ± 0.5	-10.4 ± 0.7	-0.4 ± 0.3		6.9 ± 1	15.8 ± 0.7	
COOLING (rate: 1ºC·min⁻¹)		HEATING (rate: 15ºC·min⁻¹)				
Crystallization		β' → β₁ transition and β₁ melting				
T_{onset} (ºC)		T_{onset} (ºC)				
-1.6 ± 0.6		7.2 ± 0.7				
COOLING (rate: 0.5ºC·min⁻¹)		HEATING (rate: 15ºC·min⁻¹)				
Crystallization		β' → β₁ transition and β₁ melting				
T_{onset} (ºC)		T_{onset} (ºC)				
-0.4 ± 0.5		6.9 ± 0.4				

Figure 2. SR-XRD SAXD (left) and WAXD (right) patterns of OPO corresponding to the respective DSC programs. d-spacing values (nm) are shown for the most representative peaks. a) Cooling rate: 15° C·min⁻¹; b) Cooling rate: 2° C·min⁻¹: (*) Long spacing values for some intermediate forms; c) Cooling rate: 1° C·min⁻¹; d) Cooling rate: 0.5° C·min⁻¹.

and *ex-situ* (not on-line) XRD measurements with laboratory equipment after crystallization ceased. SR-XRD can facilitate fast cooling rate measurements because of its high-intensity X-ray beam; thus, it is interesting and valuable to examine the polymorphic crystallization of multiple forms of OPO.

This study characterized the polymorphic crystallization behavior of OPO by DSC, Thermo-optical Microscopy (TOM) and SR-XRD as a function of kinetics (variation of the cooling rates).

Experimental

The 1,3-dioleoyl-2-palmitoyl glycerol (OPO) used for thermal analysis (DSC and TOM) (99% pure without further purification) was purchased from Larodan Fine Chemicals
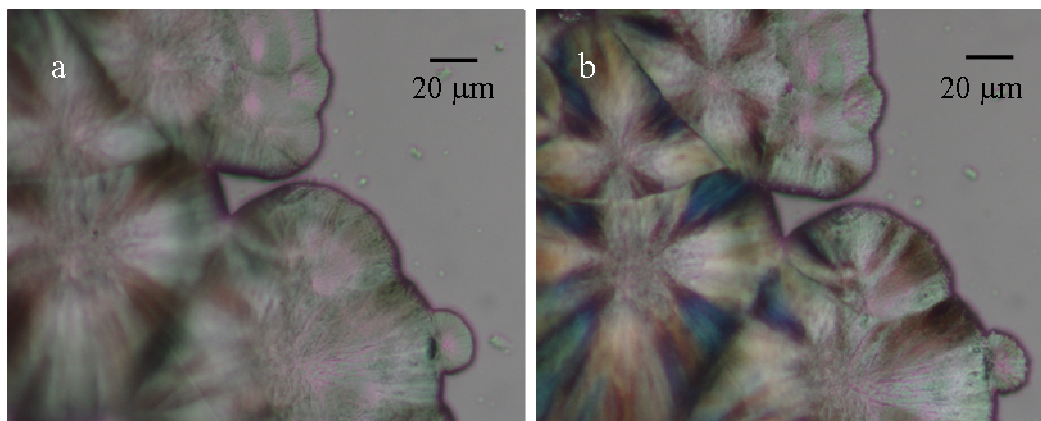
Figure 3. Thermo-optical polarized microscopy images obtained when OPO was cooled down at 2° C·min⁻¹ and heated at 15° C·min⁻¹. The temperature range corresponds to the β' → β₁ + β₂ phase transition. The colour changes become clearly noticeable. a) -14.3° C; b) 4.5° C.

(Malmö, Sweden). The 1,3-dioleoyl-2-palmitoyl glycerol used
for SR-XRD was also 99% pure and it was obtained from
Tsukishima Foods Industry (Tokyo, Japan). The DSC profiles
for both compounds were completely identical.

DSC was performed at atmospheric pressure using a Perkin-
Elmer DSC-7 calorimeter. Samples (9.0 to 9.4mg) were
weighed into 50μl aluminum pans, and covers were sealed
into place. The instrument was calibrated by reference to the
enthalpy and melting point of indium (melting temperature:
156.6ºC; ΔH_f: 28.45J·g⁻¹) and decane (melting temperature: -
29.7ºC; ΔH_f: 202.1J·g⁻¹) standards. An empty pan was used as
reference. Dry nitrogen was used as the purge gas in the DSC
cell at 23cm³·min⁻¹. Thermograms were analyzed with Pyris
Series Software to obtain enthalpy (J·g⁻¹) (integration of the
DSC signals), T_{onset} (ºC), and T_{end} (ºC) of the transitions
(intersection of the baseline and the initial and final tangent to
the transition).

Samples were cooled at different cooling rates (15ºC·min⁻¹,
2ºC·min⁻¹, 1ºC·min⁻¹ and 0.5ºC·min⁻¹) from 35ºC to -80ºC and
heated at 15ºC·min⁻¹. A minimum of three independent
measurements was made for each experiment (n = 3). Random
uncertainty was estimated with a 95% threshold of reliability
using the Student's Method, which enables estimating the
mean of a normally distributed population when the
population is small. For analysis that did not take place at a
rate of 2ºC·min⁻¹, a correction had to be made, as the DSC-7
was calibrated at the before-mentioned rate. The following
expression was applied at each value: [33]

$$T_{true} = T_{obs} - C \cdot (dT/dt)_a + C \cdot (dT/dt)_b$$

where C is a constant value (0.085), $(dT/dt)_a$ is the rate of the
analysis, and $(dT/dt)_b$ is the calibration rate (2ºC·min⁻¹).

TOM images were obtained on a Linkam THMSG-600 stage
mounted to a Nikon Eclipse 50iPol Microscope. The sample
was placed on a 7mm quartz cover slip and encased within a
pure Ag lid to ensure a uniform temperature. An LNP liquid
nitrogen cooling system and a TMS94 temperature controller
were used. Images were captured with a Nikon Digital
Camera DXM1200F and NIS-Elements Software.

SR-XRD experiments were carried out at two different
beamlines (BL-15A and BL-9C) of the SR source Photon
Factory (PF) in the National Laboratory for High-Energy
Physics (Tsukuba, Japan). For both beamlines, a double-
focusing camera operated at a wavelength 0.15nm. For BL-
9C, the X-Ray scattering data were detected by Position
Sensitive Proportional Counters (PSPCs) for the small
(SAXD) and wide angles (WAXD) simultaneously. For BL-
15A, two different detectors were used: a CCD camera for
small-angle data and PSPC for wide-angle data. The SAXD
and WAXD measurements were simultaneous. The SAXD
pattern was used for determining the chain length structure of
the triacylglycerol and the WAXD pattern permitted us to
identify the polymorphic forms[34]. The temperature program
applied to the sample was controlled by a Mettler DSC-FP84
(Mettler Instrument Corp., Greifensee, Switzerland) with
FP99 software. A 2mm-thick sample was placed in a stainless
steel sample cell with Kapton film windows. It should be
noted that the SR-XRD spectra were taken at 30s or 60s
intervals, depending on the cooling rate and the number of
transitions observed in the DSC profile.

Results and discussion

Figure 1 depicts the OPO DSC thermograms (cooling and
heating) obtained by changing the cooling rate and keeping
the same heating rate of 15ºC·min⁻¹. Table 1 specifies T_{onset}
for each transition. Crystal forms were identified by the SR-
XRD patterns of simultaneous SAXD and WAXD
measurements following the same DSC programs (Fig. 2).
Long spacing values of α, β', β₁, and β₂ forms are known
from the work of Minato et al.[12]

Cooling rate: 15ºC·min⁻¹. On cooling, the polymorphic form
that crystallizes is α (less stable). Afterwards, a solid-solid
transition takes place at -50.8 ± 1.6ºC (Table 1) to obtain
another α form (α*), characterized by an appreciable double
peak in the SAXD pattern (5.4 and 5.2nm) and a broad peak in
the WAXD pattern (0.42nm). Ueno et al.[32] reported an α form
for SOS, characterized by a double peak in the SAXD pattern
and they explained the transformation from the double SAXD
peak into a single peak (characteristic of α) as a relaxation
process of the α form. In the present work, we have called this

Table 2. Crystallographic data of the OPO polymorphic forms.

	Present work				Minato et al. work[12]		
	α	α*	β'	β₁	α	β'	β₁
Short Spacing (nm)	0.42	0.42	0.43 0.40	0.46 0.38 0.37	----	----	----
Long Spacing (nm)	5.3	5.4 5.2	4.4	6.7	4.8	4.4	6.4
Chain Length Structure	Double	Double	Double	Triple	Double	Double	Triple

form, characterized by the double SAXD peak, α*.

During the heating process, the α* form transforms into α and melts. β' then crystallizes (identified by two peaks in the WAXD pattern, with d-spacings of 0.43 and 0.40nm) and is transformed into the β₁ form (exothermic transition, see Fig. 1). Finally, the β₁ form, which is the most stable one, melts. These results are in agreement with the work of Minato et al.,[12] who studied the polymorphism of POP:OPO binary mixtures and observed the same behavior for pure OPO.

Cooling rate: 2ºC·min⁻¹. In the SAXD pattern, concurrent crystallization of α and β' forms is observed. However, on heating, the intensity of α peaks decreases, while that of β' peaks increases, possibly due to an α → β' transition. Nevertheless, in the WAXD pattern, only β' crystallization is clearly noticeable. However, the first β' peak (0.43nm) is broader than when the cooling rate is 15ºC·min⁻¹, possibly due to an overlapping of the β' first peak and a smooth α peak.

According to the DSC thermogram, on heating, a transition from β' to β₁ and β₂ must take place simultaneously, as two melting endothermic peaks are present. Nevertheless, in both the SAXD and the WAXD patterns, only the β₁ polymorphic form could be observed.

Figure 3 illustrates a thermo-optical polarized microscopy experiment using the same DSC program. In the temperature range of the solid-solid transition β' → β₁ + β₂, the sample, crystallized as spherulites, exhibited clear color changes, due to the solid-solid transition: before the transition it is possible to appreciate some brown and green colors (Figure 3a) and there are some changes to obtain some blue, yellow and brown tonalities (Figure 3b). However, it is not possible to distinguish between the newly formed β₁ and β₂ forms using this technique.

Cooling rate: 1ºC·min⁻¹. On the one hand, the SAXD pattern exhibits concurrent crystallization of α and β' forms in the cooling process, although the α peak does not become important and disappears immediately. On the other hand, the crystallization of β' is also present in the WAXD pattern, but is accompanied by some β₁ crystallization. Therefore, both SAXD and WAXD results indicate concurrent crystallization of α, β' and β₁ forms.

When the sample is heated, all β' is transformed into β₁, but before this transition, some peaks of possible intermediate forms can be seen in the SAXD profile (7.1 and 6.1nm). We must point out that only one endothermic peak with a shoulder is observed in the DSC heating thermogram, whereas the β'

→ β₁ transition should be exothermic. This may be because the β₁ melting process becomes so energetic that the convolution of both phenomena (β' → β₁ transition and β₁ melting) becomes a single endothermic peak in the DSC.

Cooling rate: 0.5ºC·min⁻¹. According to the SAXD and WAXD patterns, α does not crystallize when cooling, and there is only a concurrent crystallization of β' and β₁. Afterwards, β' transforms into β₁ on heating and β₁ melts. The DSC obtained is similar to the previous one.

In order to check the crystallization behavior at an intermediate cooling rate between 15 and 2ºC·min⁻¹, DSC experiments at a cooling rate of 8ºC·min⁻¹ and heating rate of 15ºC·min⁻¹ were carried out (not shown). The thermal profiles were similar to the one obtained by the cooling at 2ºC·min⁻¹ whose details are explained in Figure 1b.

Overall, as the cooling rate decreases, the DSC profiles become simpler. This fact is represented in the triangular shape of Table 1. Also, T_end and enthalpy values were determined for each transition, and some comparisons can be established. When the cooling rate is 15ºC·min⁻¹, α form crystallizes, giving an energetic peak; however, the α → α* transition is less energetic and much broader. Afterwards, the energy of the α melting is low when heating, and the correspondent peak becomes very narrow. The energy for the following β' crystallization and β' → β₁ transition are about the same magnitude as for the α crystallization. Finally, the β₁ melting is more energetic than all the previous phenomena, and the peaks become broader than that of the α crystallization. With cooling rates of 2º, 1º, and 0.5ºC·min⁻¹, concurrent crystallizations take place, so the processes are more complex and energies are higher (100J·g⁻¹), due to the overlapping of some phenomena, although the correspondent peaks are not so broad. The same happens during the heating step with 1 and 0.5ºC·min⁻¹: as the endothermic peak is, in fact, a convolution of the β'→β₁ transition and the β₁ melting, and energies become high. When the cooling rate is 2ºC·min⁻¹, the energy value for the transition β' → β₁ + β₂ (heating step) is similar to that for the β' → β₁ transition with a cooling rate of 15ºC·min⁻¹. Comparison of the two experiments also indicates that the energy value of the convolution of β₁ and β₂ melting (it was not possible to separate the two peaks) is the same as for β₁ melting. Therefore, it can be concluded that β₂ crystallization and melting are not as energetic as that of β₁, and the amount of β₂ crystallized is not as high. The T_onset of β₁ melting when the cooling rates are 15º and 2ºC·min⁻¹ are
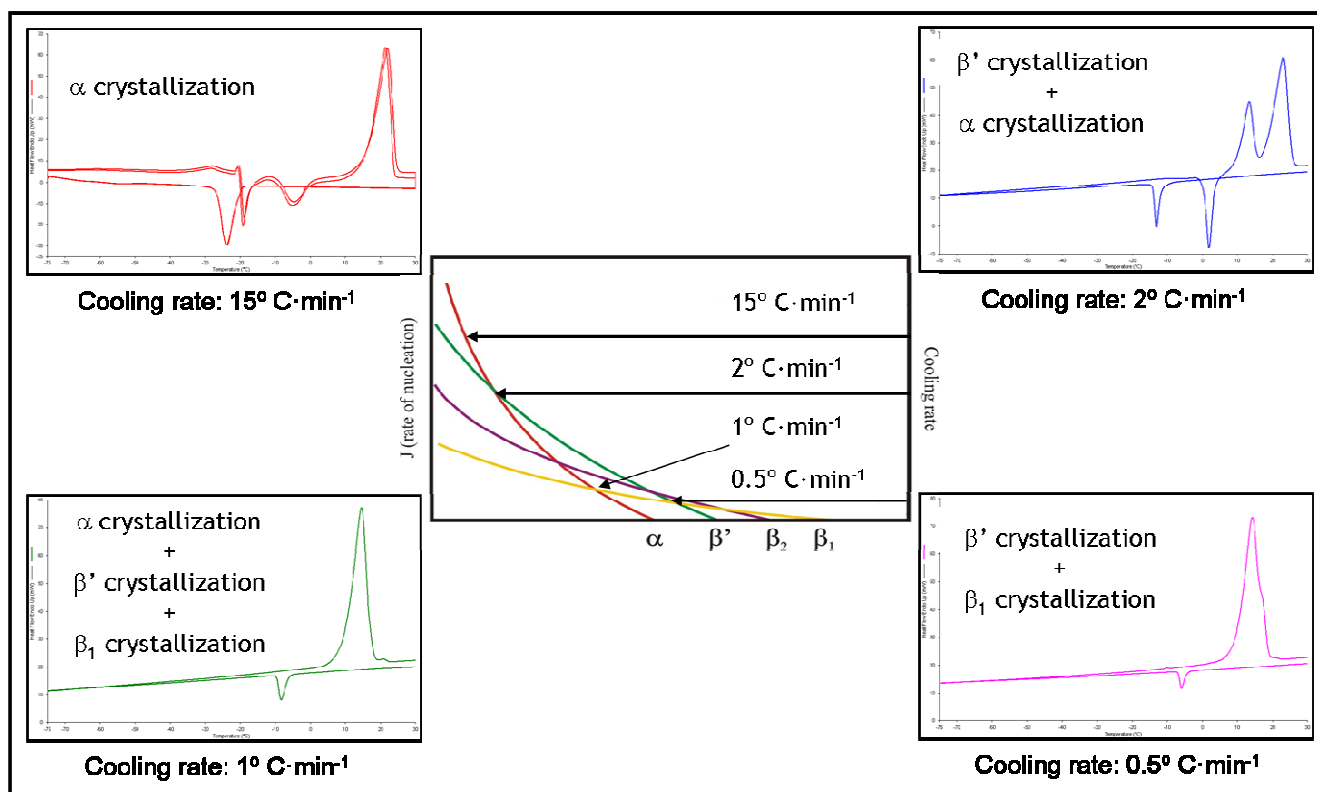
Figure 4. Diagram of the influence of changing the cooling rate on the OPO polymorphism.
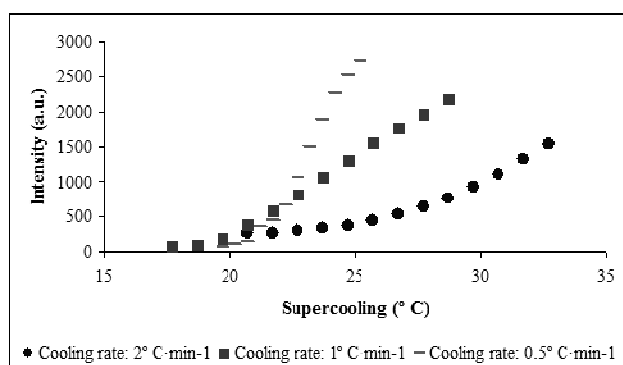
slightly different due to the fact that, at 2°C·min⁻¹, the β₁ melting peak is close to the β₂ melting peak, so the β₂ melting process makes some influence to change somehow the β₁
10 melting value. However, at 15°C·min⁻¹, the β₁ melting peak is completely isolated.

All the crystallographic data obtained in order to characterize each polymorph are summarized in Table 2, where a comparison with the Minato et al.[12] results can also be found.
15 We have defined the chain length structure of α and α* as double, although the long spacing values are higher (from 5.2 to 5.4) than those of Minato et al. As other studies have confirmed,[32] sometimes α form can reach these high values, which can be understood as a more straight double chain
20 structure.

According to the Ostwald step rule for polymorphic nucleation, the solid first formed on crystallization of a melt or a solution would be the least stable polymorph, which is first produced by spontaneous crystallization. As Ostwald
25 stated: "When leaving a given state and in transforming to another state, the state which is sought out is not the thermodynamically stable one, but the nearest in stability to the original state" and this must be the next least stable (the one with the smallest energy barrier expressed in
30 kinetic/thermodynamic terms)[4]. However, some factors (e.g., cooling rate) affect crystallization[26,27] and polymorphic nucleation. In this work, we have shown the influence of kinetics, so that as the cooling rate decreases, more stable forms crystallize, not following the Ostwald step rule. In most
35 cases, concurrent crystallizations of different polymorphs occur, but the tendency becomes clear. Therefore, this becomes an example where kinetics, thermodynamics and structural factors are competing. However, the Ostwald's Rule also states that the polymorph first formed is followed
40 successively by forms of increasing stability. This fact has been observed on the heating profiles of the experiments performed in the present work, as the phase transitions follow a sequence by continuously increasing the stability of the forms obtained. Nevertheless, further work would be required
45 to determine the effects of changing heating rates on polymorphism. Figure 4 summarizes the influence of cooling rate variation on the OPO polymorphism. The proposed diagram includes all the polymorphic sequences experimentally observed. As DSCs show, a more simplified
50 polymorphic behavior is obtained with a decreased cooling

rate because the transformation sequence becomes shorter.

Moreover, we studied the relation between the cooling and the crystallization rates of the β' form (Fig. 5). The variation of the SAXD peaks intensity of β' (at 4.5 or 4.4 nm), present during the cooling process (at three rates of cooling), is represented in front of the supercooling ($\Delta T = T_m–T_c$), in which T_m is the melting temperature of β' form and T_c becomes each experimental temperature. It was evident that the SAXD peak intensity increased more rapidly as the cooling rate decreased above the ΔT values of 22°C. Although the degree of perfection of crystals or crystallinity may vary the corresponding XRD peaks in that less perfect crystal diffract less X-ray beams, the intensity of the XRD peaks basically depends on the concentration of crystals present in the growth medium that were subjected to XRD measurement. Therefore, the results (Fig. 5) may be related to the amount of β' crystals formed during different rates of cooling. It appeared that the rate of crystallization decreased with increasing cooling rate, since the peak intensity of the SAXD pattern decreased with increasing ΔT and cooling rate. However, this was not the case. The amount of crystals is the summation of the crystallized materials in the supercooled liquid, resulting from both the rate of nucleation and subsequent crystal growth. The rate of nucleation is defined as the increase in crystal numbers per unit of time and unit of volume of supercooled liquid, and the rate of crystal growth is defined as the increase in volume of crystals per unit time. As the rate of cooling decreases, the amount of time required for the growth medium to allow crystal nucleation and crystal growth to occur increases; therefore, the integrated amount of crystals may increase with time. This phenomenon was clearly observed for the same polymorphic form of β' as depicted in Fig. 5. For example, at a supercooling value of 24 °C, the intensity values of XRD peaks obtained at the cooling rates of 2 °C/min, 1 °C/min and 0.5 °C/min are 335, 1065 and 1900, respectively. Then the times allocated for crystallization during supercooled conditions are 12 minutes (2 °C/min), 24 minutes (1 °C/min) and 48 minutes (0.5 °C/min). This result qualitatively shows the dependence of the cooling rate on the extent of crystallization due to the difference in crystallization time.

Conclusions

DSC and SR-XRD clarified the polymorphic behavior of OPO as a function of kinetics. As the cooling rate decreases, the polymorphic crystallization is directed to more stable forms, not following the Ostwald step rule. Nevertheless, concurrent crystallization often occurs in a complex phenomena. In more detail, when the cooling rate was 15°C·min⁻¹, α form crystallized; at 2°C·min⁻¹, α and β' formed; at 1°C·min⁻¹ concurrent crystallization of α, β' and β₁ occurred; and when the controlled cooling rate was 0.5°C·min⁻¹, β' and β₁ crystallized. Using SR-XRD coupled with DSC, rapid dynamic polymorphic transformations on the heating step could be identified. Also, intensities of the SAXD peaks have been related to supercooling for β' form, by comparing the slopes of the graphs obtained at each cooling rate. Results indicate that the nucleation rate of β' tends to increase as the cooling rate decreases.

Notes and references

a. Departament de Cristal·lografia, Mineralogia i Dipòsits Minerals, Facultat de Geologia, Universitat de Barcelona, Martí i Franquès s/n, E-08028 Barcelona, Spain. FAX: (+34) 934021340; TEL: (+34) 934021350; E-mail: laurabayes@ub.edu
b. Graduate School of Biosphere Science, Hiroshima University, Higashi-Hiroshima 739, Japan.

1   J. Bernstein, *Polymorphism in Molecular Crystals*, Oxford University Press, New York, USA, 2002.
2   N. Widlak, R. Hartel and S. Narine, Ed. *Crystallization and Solidification Properties of Lipids*, AOCS Press, Champaign, USA, 2001; pp 53-131.
3   W. Ostwald, *Z. Phys. Chem.* 1897, **22**, 289.
4   T. Threlfall, *Org. Process Res. Dev.* 2003, **7**, 1017.
5   D. Aquilano and G. Sgualdino, In *Crystallization Processes in Fats and Lipid Systems*; N. Garti and K. Sato, Ed.; Marcel Dekker, New York, USA, 2001; pp 1-51.
6   T. Aree, N. Chaichit and C. Engkakul, *Carbohyd. Res.* 2008, **343**, 2451.
7   D. Zhao, Y. Zhu, Q. Ruan, S. Zhang, L. Zhang, and F. Xu, *Mater. Res. Bull.* 2010, **45**, 80.
8   G. Falini, S. Fermani, M. Gazzano and A. Ripamonti, A. *Chem. Eur. J.* 1998, **4** (6), 1048.
9   A. G. Marangoni and S. S. Narine, Ed. *Physical Properties of Lipids*; Marcel Dekker, New York, USA, 2002; pp 63-217.
10   J. M. deMan, In *Physical Properties of Fats, Oils and Emulsifiers*; Widlak, N., Ed.; American Oils Chemists' Society Press, Champaign, IL, 2000; pp 79-95.
11   K. Sato and S. Ueno, In *Crystallization Processes in Fats and Lipid Systems*; N. Garti and K. Sato, Ed.; Marcel Dekker, New York, USA, 2001; pp 177-209.
12   A. Minato, S. Ueno, J. Yano, K. Smith, H. Seto, Y. Amemiya and K. Sato, *JAOCS.* 1997, **74** (10), 1213.
13   C. Akita, T. Kawaguchi and F. Kaneko, *J. Phys. Chem. B.* 2006, **110** (9), 4346.
14   K. Sato, T. Arishima, Z. H. Wang, K. Ojima, N. Sagi and H. Mori, *JAOCS.* 1989, **66**, 664.
15   J. Yano, K. Sato, F. Kaneko, D. M. Small and D. R. Kodali, *J. Lipid Res.* 1999, **40**, 140.
16   L. Zhang, S. Ueno, S. Miura and K. Sato, *J. Amer. Oil Chem. Soc.* 2007, **84**, 219.
17   A. Minato, S. Ueno, K. Smith, Y. Amemiya and K. Sato, *J. Phys. Chem. B.* 1997, **101** (18), 3498.
18   K. Sato, S. Ueno and J. Yano, *Prog. Lipid Res.* 1999, **38**, 91.
19   C. Himawan, V. M. Starov and A. G. F. Stapley, *Adv. Colloid Interfac.* 2006, **122**, 3.
20   P. Rousset, M. Rappaz and E. Minner, *JAOCS.* 1998, **75** (7), 857.
21   T. Koyano, I. Hachiya, T. Arishima, N. Sagi and K. Sato, *J. Am. Oil Chem. Soc.* 1991, **68**, 716.
22   C. L. Chong, Z. Kamarudin, P. Lesieur, A. Marangoni, C. Bourgaux, M. Ollivon, *Eur. J. Lipid Sci. Technol.* 2007, **109**, 410.
23   C. P. M. Roelands, J. H. ter Horst, H. J. M. Krammer and P. J. Jansens, *Cryst. Growth Des.* 2006, **6** (6), 1380.
24   I. Foubert, E. Fredrick, J. Vereecken, M. Sichien and K. Dewettinck, *Termochim. Acta.* 2008, **471**, 7.

25   A. G. Marangoni, T. C. Aurand, S. Martini and M. Ollivon, *Cryst. Growth Des.* 2006, **6** (5), 1199.
26   L. Bouzidi and S. S. Narine, *Langmuir.* 2009, **26** (6), 4311.
27   R. Lam, L. Quaroni, T. Pederson and M. A. Rogers, *Soft Matter.* 2010, **6**, 404.
28   G. Calliauw, V. Gibon, W. de Greyt, L. Plees, I Foubert and K. Dewettinck, *J. Am. Oil Chem. Soc.* 2007, **84**, 885.
29   R. E. Timms, *Eur. J. Lipid Sci. Technol.* 2005, **107** (1), 48.
30   K. W. Smith, In *Crystallization Processes in Fats and Lipid Systems*; N. Garti and K. Sato, Ed.; Marcel Dekker, New York, USA, 2001; pp 357-380.
31   S. Ueno, A. Minato, J. Yano and K. Sato, *J. Cryst. Growth.* 1999, **198/199**, 1326.
32   S. Ueno, A. Minato, H. Seto, Y. Amemiya and K. Sato, *J. Phys. Chem. B.* 1997, **101**, 6847.
33   Instructions Model DSC-4. Perkin Elmer, Norwalk, Connecticut, USA, (1982).
34   C. Lopez, N. Karray, P. Lesieur and M. Ollivon, *Eur. J. Lipid Sci. Technol.* 2005, **107**, 673.